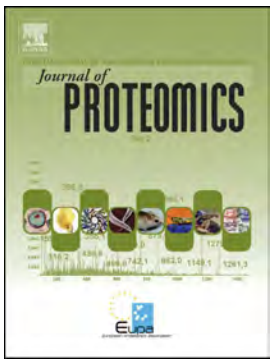

Effects of Fe and Mn deficiencies on the protein profiles of tomato (Solanum lycopersicum) xylem sap as revealed by shotgun analyses

Laura Ceballos-Laita, Elain Gutierrez-Carbonell, Daisuke Takahashi, Anunciación Abadía, Matsuo Uemura, Javier Abadía, Ana Flor López-Millán

PII: S1874-3919(17)30305-6
DOI: doi: 10.1016/j.jprot.2017.08.018
Reference: JPROT 2929

To appear in: *Journal of Proteomics*

Received date: 5 June 2017
Revised date: 19 August 2017
Accepted date: 24 August 2017

Please cite this article as: Laura Ceballos-Laita, Elain Gutierrez-Carbonell, Daisuke Takahashi, Anunciación Abadía, Matsuo Uemura, Javier Abadía, Ana Flor López-Millán , Effects of Fe and Mn deficiencies on the protein profiles of tomato (Solanum lycopersicum) xylem sap as revealed by shotgun analyses, *Journal of Proteomics* (2017), doi: 10.1016/j.jprot.2017.08.018

Effects of Fe and Mn deficiencies on the protein profiles of tomato (*Solanum lycopersicum*) xylem sap as revealed by shotgun analyses

Laura Ceballos-Laita [a], Elain Gutierrez-Carbonell [a,1], Daisuke Takahashi [b,c,2], Anunciación Abadía [a], Matsuo Uemura [c], Javier Abadía [a], Ana Flor López-Millán [d,*]

[a] *Plant Stress Physiology Group, Plant Nutrition Department, Aula Dei Experimental Station, CSIC, Apdo. 13034, 50080 Zaragoza, Spain*

[b] *United Graduate School of Agricultural Sciences, Iwate University, Morioka 020-8550, Japan*

[c] *Cryobiofrontier Research Center, Faculty of Agriculture, Iwate University, Morioka 020-8550, Japan*

[d] *USDA-ARS Children's Nutrition Research Center, Department of Pediatrics, Baylor College of Medicine, 1100 Bates St., Houston, TX 77030, USA.*

*Corresponding author

email address: anaflorlopez@gmail.com

[1] Current address: SCIEX S.L. Calle Valgrande 8, Alcobendas, 28108 Madrid, Spain.

[2] Current address: Central Infrastructure Group Genomics and Transcript Profiling, Max-Planck-Institute of Molecular Plant Physiology, Am Mühlenberg 1, 14476, Postdam, Germany.

Running tittle: Xylem sap shotgun proteomics from Fe- and Mn-deficient tomato plants

ABSTRACT

The aim of this work was to study the effects of Fe and Mn deficiencies on the xylem sap proteome of tomato using a shotgun proteomic approach, with the final goal of elucidating plant response mechanisms to these stresses. This approach yielded 643 proteins reliably identified and quantified with 70% of them predicted as secretory. Iron and Mn deficiencies caused statistically significant and biologically relevant abundance changes in 119 and 118 xylem sap proteins, respectively. In both deficiencies, metabolic pathways most affected were protein metabolism, stress/oxidoreductases and cell wall modifications. First, results suggests that Fe-deficiency elicited more stress responses than Mn deficiency, based on the changes in oxidative and proteolytic enzymes. Second, both nutrient deficiencies affect the secondary cell wall metabolism, with changes in Fe deficiency occurring *via* peroxidase activity, and in Mn deficiency involving peroxidase, Cu-oxidase and fasciclin-like arabinogalactan proteins. Third, the primary cell wall metabolism was affected by both nutrient deficiencies, with changes following opposite directions as judged from the abundances of several glycoside-hydrolases with endo-glycolytic activities and pectin esterases. Fourth, signaling pathways *via* xylem involving CLE and/or lipids as well as changes in phosphorylation and N-glycosylation also play a role in the responses to these stresses.

Keywords: Iron deficiency; Mn deficiency; Proteomics; Shotgun; Tomato; Xylem sap.

1. Introduction

The xylem is a key component of the vascular transport system of land plants, essential for long- and short-distance transport and distribution of nutrients and signals. The major role of the xylem is to transport water and mineral nutrients from roots to shoots. The flow of the fluid through the treachery elements that compose the xylem vessels, known as xylem sap, is mainly driven by the negative pressure created by transpiration, whereas differences in water potential between the soil and the root system can also create a positive root pressure that contributes to the xylem sap flow [1].

The xylem sap is mainly composed by water and mineral nutrients, but also contains a wide array of other minor compounds, including carbohydrates, hormones, secondary metabolites, polyamines, amino acids, peptides and proteins [2-9]. In spite of the fact that the treachery elements that compose the xylem have lost their nuclei and cellular content during differentiation and are therefore unable to synthesize proteins, the xylem sap has been widely reported to have a characteristic protein profile [7, 10-12]. Many of the xylem sap proteins contain predicted N-terminal signals and are synthetized in the roots and subsequently loaded in the xylem sap via the secretory pathway [8, 13-15], whereas others may arise from cytoplasmic contamination from neighboring tissues [7].

Proteomic studies have allowed generating a detailed xylem sap protein repertoire. Since one of the major limitations for these studies is the low protein concentration present in xylem sap, which ranges between 10 and 300 μg mL^{-1} (see [7] for a review), initial studies performed by means of one dimensional electrophoresis only provided a limited number of protein species [10]. Later on, the development of more sensitive high-throughput proteomic techniques allowed to decipher in detail the xylem sap proteome of a significant number of plant species, including

tomato (see [7] for a review). A comprehensive analysis of these proteomes, which included between 100 and 500 proteins, indicated that the major functional category in the xylem is polysaccharide metabolism, including mainly cell wall hydrolases [2, 7, 12]. The xylem proteome, as it also occurs in other plant fluids, contains a battery of proteins related to redox homeostasis, plant defense and proteases, which are thought to constitute a local defense barrier against biotic and abiotic stresses [7, 16-19].

The xylem sap also participates actively in the root to shoot signaling pathway that helps regulating vegetative growth depending on the root environment conditions [20]. In situations such as plant-symbiotic associations or nutrient deficiencies, the xylem serves as a conduit for signaling metabolites [20, 21], with many of them being hormones. For instance, in P- and N-deficient conditions xylem-mobile cytokinins regulate the nutrient starvation response [22-28]. Interestingly, the xylem sap proteome also contains a small number of proteins involved in regulatory processes that could participate in root to shoot signaling, including transcription factors, fasciclin-like arabinogalactan proteins and kinases [2, 7, 29-31].

Minerals such as Fe and Mn are essential micronutrients for living organisms including plants [32, 33]. Both metals are cofactors for numerous enzymes and play important roles in photosynthesis, with Mn being required in the catalytic center of the oxygen evolving complex [33-36] and Fe participating in electron transfer reactions of the photosynthetic apparatus as well as in the synthesis of chlorophyll [37-39]. Deficiencies of both nutrients often occur in alkaline soils where there is limited availability of metals, leading to reduced growth and yield and affecting the nutritional quality of plant crops [32, 33, 35, 40-43]. In the xylem sap, Fe is found complexed with carboxylates [44, 45] whereas it has been estimated that 60% of the xylem Mn is in the form of Mn^{2+} [46]. In spite of the fact that proteins are unlikely to play a direct role in the

transport of these metals in the xylem, they might play important roles in root to shoot nutrient signaling and protection against metal-induced ROS, among others. Comparative proteomics can provide useful information not only about processes occurring in xylem sap during the adaptation to nutrient stresses, but also can help to target proteins putatively involved in systemic regulation for future studies [47, 48]. A significant number of proteomic studies have focused into the effect on different sub-proteomes of nutrient stresses such as Fe (see [49, 50] for reviews) and Mn [51, 52], but the number of proteomic studies devoted to the effect of nutrient deficiencies and/or toxicities in the xylem sap has been limited, to the best of our knowledge, to studies on the effects of salt stress, K deficiency and N starvation or overload [53-55].

Therefore, the aim of this work was to study the effects of Fe and Mn deficiencies on the protein profile of the xylem sap of tomato (*Solanum lycopersicum*), with the aim of elucidating plant response mechanisms to these nutritional stresses. Tomato was chosen as a model plant because the tomato genome has been published and this plant species has adequate root pressure and turgid stems that permit xylem sap sampling in sufficient amounts by de-topping. The high-throughput shotgun analysis has permitted to identify and quantitate a large number of low abundance proteins in the tomato xylem sap.

2. Materials and methods

2.1. Plant material and xylem sap collection

Tomato (*Solanum lycopersicum*, cv. Tres Cantos) plants were grown hydroponically in a controlled environment chamber (Fitoclima 10.000 EHHF, Aralab, Lisbon, Portugal) with a photosynthetic photon flux density (PPFD) of 400 µmol m^{-2} s^{-1} photosynthetically active radiation, 80% relative humidity and a photoperiod of 16 h, 23ºC/8 h, 18ºC day/night regime. In

the Fe deficiency experiment, seeds were germinated in vermiculite for 13 days in half-strength Hoagland nutrient solution containing 45 μM Fe-EDTA and 4.6 μM $MnCl_2$. Seedlings were then transplanted to 10 L plastic buckets (16-18 plants per bucket) containing half-strength Hoagland nutrient solution and grown for an additional 13-day period. After this time, solutions were renewed and control (45 μM Fe(III)-EDTA, 4.6 μM $MnCl_2$) and Fe-deficiency treatments (0 μM Fe(III)-EDTA) imposed. In the Mn experiment the time line and experiment design (including control conditions) were the same, but Mn-deficient plants (0 μM $MnCl_2$) were germinated and grown without Mn and with 45 μM Fe(III)-EDTA throughout the experiment. Plants were analyzed and xylem sap collected eight days after treatment onset. At this time, plants were de-topped approximately 5 mm above the mesocotyl using a carbon steel disposable scalpel (Nahita, Beriain, Spain) and the exudate fluid was collected from the cut surface. The initial sap collected during the first 5 min was discarded to minimize contamination with other plant fluids and broken cells, and then the xylem sap was collected for 30 min using a micropipette tip. Samples were kept on ice during the entire collection period.

2.2. Experimental design

The experiment was repeated six times with independent batches of plants. Each batch of plants consisted of one 10-L bucket per treatment with 16-18 plants per bucket. In each batch of plants, the xylem sap fluid from all plants in a given treatment was pooled together and considered as a biological replicate (n = 6).

2.3. Mineral analysis and chlorophyll estimation

The concentration of micronutrients (Fe, Mn, Cu and Zn) in the collected fluid was determined by ICP-MS (Inductively Coupled Plasma Mass Spectrometry; model Agilent 7500ce; Agilent

Technologies, Tokyo, Japan) after digestion with 1% HNO_3 (TraceSELECT Ultra, Sigma-Aldrich, Madrid, Spain).

Leaf chlorophyll content was estimated using a SPAD 502 apparatus (Minolta Co., Osaka, Japan). The SPAD values of young and old expanded leaves were recorded at sampling time (8 days after treatment onset) and an average per treatment obtained.

2.4. Protein Extraction

Proteins in the collected fluid were precipitated immediately by adding five volumes of cold 0.1 M ammonium acetate in methanol, containing 0.07% β-mercaptoethanol. Samples were kept overnight at -20ºC and then centrifuged at 20,000 x*g* for 20 min. The pellet was washed twice with cold methanol, dried with N_2 gas and solubilized in a sample rehydration buffer containing 8 M urea, 2% (w/v) CHAPS, 50 mM DTT, 2 mM PMSF and 0.2% (v/v) IPG buffer pH 3-10 (GE Healthcare, Uppsala, Sweden). After rehydration, samples were incubated in a Thermomixer comfort device (Eppendorf AG, Hamburg, Germany) at 42 ºC and 1,000 rpm during 3 h, then centrifuged at 10,000 x*g* for 10 min at RT and filtered (0.45 µm ultrafree-MC filters, Millipore, Bedford, USA). Protein concentration in the samples was quantified immediately with the Bradford method using an Asys UVM 340 spectrophotometer with microtiter plates (Biochrom Ltd., Cambridge, UK) and BSA as standard.

2.5. Label free liquid chromatography-tandem mass spectrometry (LC- MS/MS)

Sample preparation for label free LC-MS/MS was carried out according to [56]. Briefly, 5 µg of total proteins were subjected to 1-DE to remove non-protein compounds. The resulting gel bands were cut into six pieces, proteins were *in gel* digested with trypsin, and peptides were subsequently extracted.

Peptide solutions were concentrated in a trap column (Lcolumn Micro 0.3 x 5 mm; CERI, Japan) using an ADVANCE UHPLC system (Michrom Bioresources, Aubum, CA, U.S.A.). Elution was carried out with 0.1% (v/v) formic acid in ACN and concentrated peptides were separated in a Magic C_{18} AQ nano column (0.1 x 150 mm; Michrom Bioresources) using a linear gradient of ACN (from 5 to 45%) and a flow rate of 500 nL min^{-1}. Peptide ionization was carried out with a spray voltage of 1.8 kV using an ADVANCE spray source (Michrom Bioresources). Mass spectrometry analysis was carried out on an LTQ Orbitrap XL (Thermo Fisher Scientific, Waltham, MA, U.S.A.) equipped with Xcalibur software (v. 2.0.7, Thermo Fisher Scientific) and mass data acquisition parameters were set as described elsewhere [57].

Mass data analysis was performed according to [58]. Protein identification was carried out using the full peptide list with the Mascot search engine (version 2.4.1, Matrix Science, London, U.K.) and NCBI 20141009 database (50,750,890 sequences; 18,190,226,827 residues). Search parameters were: peptide mass tolerance ± 5 ppm, MS/MS tolerance ± 0.6 Da, one allowed missed cleavage, allowed fixed modification carbamidomethylation (Cys), and variable modification oxidation (Met) and peptide charges were set to +1, +2 and +3. Positive protein identification was assigned with at least two unique top-ranking peptides with scores above the threshold level ($p \leq 0.05$). Protein information was exported from Mascot .xml format and imported to Progenesis software (v. 2.0, Nonlinear Dynamics, Newcastle upon Tyne, U.K.), which then associate peptide and protein information. The MS proteomics data have been deposited to the ProteomeXchange Consortium *via* the Pride partner repository with the data set identifier PXD007517.

To assess the effect of Fe and Mn deficiencies in the protein profile of tomato xylem sap, we calculated the ratio of normalized protein abundance between the Fe-deficient or Mn-deficient

and the control samples. Only changes with a $p \leq 0.05$ (ANOVA) and a normalized abundance ratio ≥ 2 or ≤ 0.5 were considered as statistically significant and biologically relevant, respectively. Multivariate statistical analysis (Principal Component Analysis; PCA) was carried out using SPSS Statistical software (v. 24.0), including only proteins showing statistically significant changes (ANOVA; $p < 0.05$) as a result of the Fe-deficiency and Mn-deficiency treatments.

We used the GO biological process annotation (http://www.geneontology.org) and domain annotations for classification of each individual protein identified into nine functional categories (proteolysis, protein synthesis, polysaccharide related, stress/oxido-reductases, lipid metabolism, carbohydrate metabolism, signaling, unknown and a miscellaneous group containing functional categories not belonging to the previous groups). The presence of signal peptides in proteins was assessed using TargetP (www.cbs.dtu.dk/services/TargetP) [59], and SecretomeP (www.cbs.dtu.dk/services/SecretomeP) was used to assign proteins to secretory classical and non-classical classes [60, 61].

3. Results

3.1. Plant material and xylem sap collection

Tomato plants grown without Fe showed deficiency symptoms as soon as five days after the treatment onset. At sampling time (eight days) a marked chlorosis of the younger leaves was observed (Figures 1 and 2 in Ref [62]), as indicated by the SPAD reading in these plants (13.6) which was significantly lower than that measured in control plants (42.4) (Table 1). Accordingly, the Fe concentration in the xylem sap of Fe-deficient plants was 15.5 μM, 68% lower than that found in xylem sap from control plants, whereas no significant differences were observed in the concentrations of Mn, Cu and Zn (Table 1).

To achieve Mn-deficiency, plants were grown without Mn from germination. At sampling time, both old and young leaves in Mn-deficient plants showed interveinal chlorosis with a "checkered" pattern (Figures 1 and 2 in Ref [62]). The SPAD value of Mn-deficient plants (29.6) was 30% lower than those of control plants (Table 1). The concentration of Mn in xylem sap of deficient plants was almost 10 times lower than that in control plants (0.7 vs. 6.5 μM). The concentration of Fe in the xylem sap was also 44% lower in Mn-deficient (26.6 μM) that in control plants (47.8 μM), but still significantly higher than that in Fe-deficient plants (Table 1). No significant changes were detected in the xylem sap concentrations of Cu and Zn (Table 1).

Xylem bleeding rates were similar in control and Fe-deficient plants (approximately 0.8 mL $plant^{-1}$ h^{-1}), whereas in the Mn-deficient plants this rate was 38% higher (1.1 mL $plant^{-1}$ h^{-1}) (Table 1). Protein extraction yields were also similar in control and Fe-deficient plants, in the range from 6.9 to 9.0 ng protein μL^{-1}, whereas values in the Mn deficient xylem sap were 53% lower (4.2 ng protein μL^{-1}) than those in the controls (Table 1).

3.2. Identification of xylem sap proteins

The LC-MS/MS analysis detected 1534 proteins in the tomato xylem sap, and 643 of them were reliably identified and quantified with at least two peptides and therefore considered in this study. The lists of peptides detected and proteins identified and quantified are shown in Tables 1 and 2 in Ref [62], respectively. The large majority of protein species identified and quantified (84%; 542) were identified as pertaining to the *Solanum* genus, with 94% of them (509) matching specifically to the species *S. lycopersicum* (Table 2 in Ref [62]).

The PCA analysis of the statistically significant changes (ANOVA; $p<0.05$) showed a good separation between treatments, with the first and second components explaining approximately 74 and 11% of the variation, respectively (Figure 3 in Ref [62]).

The prediction programs TargetP and SecretomeP indicated that a high percentage (66%; 425 proteins) of the 643 identified and quantified proteins can be assigned to the secretory pathway. Among these secretory proteins, 223 (35% of the total identified in the xylem sap) were classified as classical secretory (CS) (containing peptide signals) whereas 202 (31%) were classified as non-classical secretory (NCS). The remaining 218 proteins (34%) were predicted as non-secretory, and therefore their presence in the xylem sap deserves further studies, since it possibly reflects some degree of contamination (see [7] for a discussion on this topic).

3.3. Effect of Fe-deficiency on the xylem sap proteome

A volcano plot, showing the relationship between statistical significance [$-\log_{10}$(p-value)] and biological significance [$\log_2$(fold-change)], was used to describe the changes induced by Fe deficiency on the xylem sap proteome (Fig. 1). Iron deficiency caused statistically significant (ANOVA, $p \leq 0.05$) and biologically relevant (fold ≥ 2 or fold ≤ 0.5) changes in 119 proteins (Fig. 1). All these proteins are presented in Table 3 in Ref [62], and those exhibiting large changes in abundance (fold > 5 or < 0.2) are shown in Table 2.

Among them, 54 proteins showed relative decreases (green dots in Fig. 1A), and from these 35 were classified as secretory (10 CS and 25 NCS; Fig. 1B; Table 3 in Ref [62]). The remaining 19 proteins (35%) were classified as non-secretory and therefore excluded from the biological interpretation (Table 3 in Ref [62]). Functional classification of the 35 secretory proteins decreasing in abundance revealed that protein metabolism (17%) and stress/oxido-reductases

(17%) were the most represented categories, whereas the remaining proteins were classified into a wide variety of miscellaneous categories (Fig. 1D; Table 3 in Ref [62]). Interestingly, proteins involved in polysaccharide metabolism were not found among those decreasing in abundance (Fig. 1D; Figure 3B). Overall, decreases were moderate (between 50 and 70%) and only one CS protein, a peroxidase (AtPER44-like; K4D7T6) decreased more than 80% as a result of Fe deficiency (Table 2; Table 3 in Ref [62]).

Iron deficiency caused relative increases in the abundance of 65 proteins (red dots in Fig. 1A) and from these 53 were classified as secretory proteins (44 CS and 9 NCS; Fig. 1C; Table 3 in Ref [62]). The remaining 12 proteins (18%) were classified as non-secretory and therefore excluded from the biological interpretation (Table 3 in Ref [62]). Functional classification of the 53 secretory proteins increasing in abundance revealed that protein metabolism (proteolysis and protein synthesis; 28%), polysaccharide metabolism (26%), and stress/oxido-reductase proteins (13%) were the most represented categories (Fig. 1E; Fig. 3B). Remarkable increases in abundance (higher than 10-fold) were observed in eight proteins classified as CS. Three of them increased more than 30-fold, including two leucine rich-repeat (LRR) receptor-like kinases (K4B2Y3 and K4D0Y5) involved in regulation and a GDSL esterase/lipase (K4DD79) classified in the lipid metabolism category (Table 2; Table 3 in Ref [62]). Five of them increased between 10- and 20-fold, including a protease inhibitor similar to miraculin (K4C8U3), a predicted basic 7S globulin with an aspartic peptidase domain (K4AXP3), a beta-glucosidase 8 from the glycoside hydrolase (GH) family 17 (B5M9E5), a peroxidase (AtPER72-like; K4BFP3), and a nutrient reservoir protein similar to conglutin (K4CP48) (Table 2; Table 3 in Ref [62]). Furthermore, eight more proteins, mostly involved in catabolic processes, presented 5- to 10-fold increases, and these included three proteases (two aspartic proteases and a MEROPS family S8

peptidase), two acid phosphatases, a GH-18 family protein, a peroxidase-52 like protein, and an uncharacterized protein (Table 2). Except for the NCS MEROPS family S8 peptidase (O82777), all were classified as CS proteins (Table 2).

3.4. Effect of Mn-deficiency on the xylem sap proteome

Manganese deficiency caused significant (ANOVA, $p \leq 0.05$) and biologically relevant (fold ≥ 2 or fold ≤ 0.5) changes in 118 proteins of the xylem sap proteome (Fig. 2). All these proteins are presented in Table 4 in Ref [62], and those exhibiting large changes in abundance (fold > 5 or < 0.2) are shown in Table 3.

Among them, 76 proteins showed relative decreases in abundance (green dots in Fig. 2A), and from these 67 were classified as secretory (53 CS and 14 NCS; Fig. 2B; Table 4 in Ref [62]). Only 9 proteins (12%) decreasing in abundance were classified as non-secretory and therefore excluded from the biological interpretation (Table 4 in Ref [62]). Functional classification of the secretory proteins decreasing in abundance with Mn deficiency revealed that protein metabolism (proteolysis and protein synthesis; 24%), polysaccharide metabolism (19%) and stress (19%) were the most represented categories (Fig. 2D; Figure 3B). Among them, the largest decrease (99%) was found in two CS proteins, the endonuclease 1 (G3XKQ7) and a predicted LRR receptor-like kinase (K4B2Y3) (Table 3; Table 4 in Ref [62]). Interestingly, both proteins increased in Fe-deficient xylem sap, with the latter being among those proteins showing the largest increases (Table 2; Table 3 in Ref [62]). Six more CS proteins presented considerable decreases (between 80 and 90%) including two purple acid phosphatases (K4D9N7 and K4DC68), a predicted subtilisin from the MEROPS peptidase family S8 (K4D3L8), the subunit L17 of the 60S ribosomal complex (K4CUW3) and two uncharacterized proteins (K4CGQ4, K4D0G7) (Table 3; Table 4 in Ref [62]).

Manganese deficiency caused relative increases in the abundance of 42 proteins (red dots in Fig. 2A) and from these only 15 were classified as secretory proteins (3 CS and 12 NCS; Fig. 2C; Table 4 in Ref [62]). The remaining 27 proteins, accounting for a high percentage (64%) of the identified proteins, were classified as non-secretory and therefore excluded from the biological interpretation (Table 4 in Ref [62]). Functional classification of the 15 secretory proteins showing increases in abundance revealed that carbohydrate metabolism (33%, 5 proteins) was the most represented category (Fig. 2E). The remaining proteins were distributed among unknown (three proteins), proteolysis and stress with one protein each, and in a miscellaneous group (five proteins involved in amino acid metabolism and ATP hydrolysis coupled to proton transport) (Fig. 2E; Figure 3B). Most increases were moderate, ranging between 2- and 3-fold (Table 4 in Ref [62]). The most remarkable increases measured in Mn-deficient xylem sap (> 5 fold) corresponded to a regulatory subunit of the chloroplastic ATP synthase (7-fold; Q2MIB5) and to two uncharacterized proteins containing LRR (14-fold; K4CHI8) and NAD(P)-NAD(P) binding Rossmann (7-fold; K4B0S2) domains (Table 3).

3.5. Comparison of the changes observed in secretory proteins in both nutrient deficiencies

The comparison between secretory proteins showing significant and biologically relevant changes in Fe- and Mn-deficient conditions (88 and 82 proteins, respectively; Fig. 3A) revealed that there were metabolic categories, including protein and polysaccharide metabolisms and stress/oxido-reductases, which clearly followed a different trend depending on the specific nutrient deficiency (Fig. 3B). When considering the 24 secretory proteins changing in relative abundance in both nutrient deficiencies (20 CS and 4 NCS) (Table 4; Fig. 3A and Fig. 3C), all of them decreased as a result of Mn deficiency, whereas in Fe deficient xylem sap only eight of them decreased (Fig. 3C, Table 4). Proteins in the protein and polysaccharide metabolism

categories followed opposite trends (as occurred when all proteins changing in abundance were compared; Fig. 3B), with most proteins increasing in Fe-deficient and decreasing in Mn-deficient xylem sap (Fig. 3C). A similar behavior was observed in the miscellaneous group of proteins. On the other hand, the categories of lipid- and stress/oxido-reductase showed a similar behavior in both deficiencies, with the majority of proteins decreasing (Fig. 3C).

Proteins showing opposite changes in abundance included three structural components of the ribosome and two aspartic proteases in the protein metabolism category, two hydrolases from families GH16 and 17, a SGN-hydrolase and a pectin esterase inhibitor in the polysaccharide metabolism category, and a miscellaneous group containing seven proteins (three acid phosphatases, a LRR receptor-like kinase, a nectarin-1, an endonuclease 1 and an uncharacterized protein) (Table 4). The most remarkable change in these groups was measured in the LRR receptor-like kinase which, as commented above, was highly increased (33-fold) in Fe-deficient xylem sap and almost disappeared in Mn-deficient conditions.

Proteins decreasing in both treatments included three peroxidases (AtPER14, 12- and 52-like), three proteases from the MEROPS peptidase families S8, 10 and A1, a lipid domain (PI-PLC X) containing protein and an uncharacterized protein (Table 4).

4. Discussion

The proteomic approach used in this study has allowed for the reliable identification and quantification of a large set of proteins in the xylem sap (643). This number is slightly higher than those found in other xylem sap studies with LC-MS/MS [12, 31] and considerably higher than those found with 2-DE (100-200 proteins; [7], highlighting the sensitivity of the methodological approach used. Approximately 67% of the identified xylem proteins (425) were

classified as secretory using prediction tools, a percentage lower than those reported, using a similar shotgun approach, in *Brassica oleracea* (87%; [12]) and *Gossypium hirsutum* (90%; [31]). Approximately one third of the identified and quantified proteins were not considered in the biological interpretation of the results, since they were classified as non-secretory and thus could reflect cytoplasmic contamination. The higher percentage of non-secretory proteins found here may also be ascribed to the high sensitivity of the LC-MS/MS approach utilized, although their unequivocal assignment to the xylem sap proteome would require further studies.

Both micronutrient deficiencies caused significant and biologically relevant changes in a similar number of secretory proteins, accounting for approximately 20% of the secretory xylem sap proteome. This percentage is within the ranges reported for the effects of Fe-deficiency on other sub-proteomes [49] and somewhat higher than those reported for Mn-deficient plants [63, 64]. Manganese deficiency caused decreases in abundance in most of the xylem secretory proteins changing in abundance (82%; 67 proteins), whereas only 40% (35 proteins) decreased in abundance as a result of Fe deficiency (Figure 3B). Overall, these results, along with the protein concentration changes observed (Table 1) indicate that Fe and Mn shortage increased and decreased, respectively, the xylem sap protein load. This would be in agreement with the opposite changes observed with both stresses in ribosomal proteins and certain proteases that can putatively be involved in protein maturation (Table 4). Furthermore, since the xylem sap exudation rate in Mn deficient plants was higher than those in Fe-deficient and control plants, the Mn deficiency-induced decreases in protein abundances would be even more marked if changes were compared on a xylem sap volume basis instead of on a protein basis.

4.1. The xylem sap proteome of manganese deficient plants is less proteolytic than that of iron deficient plants

Among the secretory proteins affected in abundance by Fe and Mn deficiencies (88 and 82 proteins, respectively) a large number (15 and 13 proteins, respectively) were related to proteolysis. However, whereas the large majority of proteins affected by Fe deficiency (11 proteins) increased in abundance (Table 3 in Ref [62]; Fig. 3B), Mn deficiency caused decreases in the relative abundance of all but one of these proteins (Figure 3B). Proteins increasing upon Fe deficiency included five aspartic proteases (MEROPS family A1), three subtilisin-like serine peptidases (MEROPS family S8), one serine carboxypeptidase (MEROPS family S10) and two protease inhibitors (MEROPS inhibitor family I3 and I20). Five of these proteins (Table 2) presented abundance increases among the largest measured in this study (between 5- and 21-fold). The peptidases decreasing with Mn deficiency were similar to those found in Fe-deficient xylem sap and included four aspartic proteases (MEROPS family A1), four subtilisin-like serine peptidases (MEROPS family S8), three serine carboxypeptidase (MEROPS family S10) and a glycopeptide hydrolase (PNGase A). The only protease increasing with Mn deficiency was a non-classical secretory processing metalloprotease (MEROPS family M16) that is likely to be mitochondrial. Among these proteins, a subtilisin-like protein (K4D3L8) showed one of the largest decreases measured (87%). These specific groups of proteases have been consistently found in xylem sap, where they play roles in the degradation of damaged proteins and signaling, and also constitute a defense mechanism against pathogen infection [7].

The increases in proteases abundance upon Fe deficiency may suggest that they are needed to mediate degradation of ROS-damaged proteins, since it is known that Fe deficiency increases oxidative stress [65, 66]. On the other hand, the decreases measured in Mn-deficient plants

support that the environment of Mn-deficient xylem sap is less proteolytic and therefore it can be hypothesized that damaged proteins are less abundant under Mn deficiency than under Fe deficiency or control conditions. However, not all the proteases increased upon Fe shortage (four of them decreased) and protease inhibitors significantly increased in abundance, suggesting that creating a proteolytic environment for damaged protein degradation or defense is not the only role of the proteins found in this category in the Fe-deficient xylem sap, with other additional roles being likely. For instance, proteases may be needed for maturation of cell wall proteins [67], and in *Arabidopsis* it has been described that some extracellular aspartic proteases can generate peptide elicitors, mediating a signaling system involved in the activation of local and systemic defense responses against biotic stresses [19]. Indeed, three aspartic proteases were affected by both nutrient deficiencies (one decreasing in both cases and two increasing or decreasing with Fe or Mn deficiency, respectively; Table 4). Taken together with the changes of LRR-RLKs (commented below in section 4.4), it is tempting to speculate that a similar peptide signaling system may also occur in nutrient deficiencies. Finally, the decrease in proteases upon Mn shortage could also indicate that maturation of secreted proteins is not needed, in line with the very low percentage (18%) of secretory proteins increasing under Mn deficiency.

4.2. The xylem sap proteome of iron-deficient plants shows more protection against oxidative stress than that of manganese-deficient plants

The stress category (including oxido-reductases and defense proteins) was largely affected by Fe and Mn deficiencies (13 and 14 proteins, respectively). However, while Fe deficiency caused both, increases and decreases in protein abundance (seven and six proteins, respectively), Mn deficiency caused decreases in abundance in all but one protein. Most of the proteins in this category corresponded to oxido-reductases, but the subcategories affected were slightly different

depending on the specific nutrient stress, with Fe deficiency inducing changes mostly in class III heme-binding peroxidases (five decreasing and four increasing), and Mn deficiency causing decreases in Cu oxidases (five proteins) and peroxidases (three proteins).

The peroxidases decreasing in abundance in both deficiencies were similar, and among them we found orthologues of the *Arabidopsis* AtPrx 12, 44, 52 (in both deficiencies) and AtPrx 53 (only in the case of Fe deficiency) (Tables 3 and 4 in Ref [62]). All but AtPrx44, which has an unknown specificity, are known to be involved in lignin formation and their activities affect lignin content, structure and composition [68-70]. Therefore, these decreases support that the lignin composition of the secondary cell wall is affected similarly by both nutrient deficiencies. However, four more peroxidases also increased in Fe-deficient xylem sap, and they were similar to AtPrx 21, 52, 63 and 72. Two of them (AtPrx52 and 72) are involved in lignin synthesis, one has an unknown specificity and one (AtPrx21) has been described as a defense protein [71]. These results indicate that the effect of Fe deficiency on the secondary cell wall *via* peroxidase activity is more marked than that of Mn deficiency, and furthermore reveal the complexity of the changes, since some lignin-related peroxidases increased and some decreased. It is remarkable that the availability of Fe does not seem to play a direct role in the abundance of these heme-binding peroxidases. In addition, the peroxidases increasing in abundance can also have a role protecting from Fe-deficiency induced oxidative stress. The existence of oxidative stress is also supported by the increase measured in a predicted nectarin-1, (K4B1G7), a Mn binding germin likely having MnSOD activity [72], which is likely to protect from oxidative stress while providing the substrate for the peroxidases. In the Mn-deficient xylem sap this nectarin decreased in abundance, reflecting the Mn shortage.

Manganese deficiency also caused decreases in five Cu-oxidases, including three blue-copper proteins of unknown function, with one cupredoxin and one phytocyanin domain, as well as two multi-copper oxidoreductases. These decreases might indicate changes in the redox state of the xylem sap towards a less oxidative environment, although the decrease in the predicted laccase (K4C1R5), which plays a role in lignin polymerization [73], may also affect the structure of the secondary cell wall. Two more proteins decreasing upon Mn deficiency were a predicted gamma-glutamyltranspeptidase 3-like (K4DBV2), whose *Arabidopsis* orthologue has been described as a cell wall associated protein that prevents oxidative stress by removing oxidized glutathione [74, 75], and a L-gulonolactone oxidase-like, which catalyzes the synthesis of ascorbic acid [76]. These decreases in antioxidant enzymes also support that the environment in the Mn-deficient xylem is less oxidative than in control plants.

Overall, the changes in abundance of oxidative and proteolytic enzymes, which increase in Fe deficiency and decrease in Mn deficiency (Figure 3B), indicate that Fe-deficiency elicits more stress responses in the xylem sap than Mn deficiency. In addition, changes in oxido-reductases related to lignin metabolism (which are similar to those measured in GHs; see section 4.2) suggest differences in the secondary cell wall composition between Mn-deficient and Fe-deficient plants that could be mainly attributed to peroxidases in the case of Fe deficiency, and peroxidase, copper-oxidase and fasciclin-like arabinogalactan proteins (see section 4.2) in the case of Mn deficiency.

4.3. Iron and manganese deficiencies affect primary cell wall metabolism in an opposite manner

Iron and Mn deficiencies elicited a marked activation and deactivation, respectively, of the primary cell wall metabolism. A large number of proteins (14) involved in polysaccharide metabolism increased in abundance with Fe deficiency (Figure 3B), including 10 glycoside

hydrolases (GH; families GH- 5, 16, 17, 18, 19 and 20), two pectic modifying enzymes (K4D4J5 and K4D0N0), a rhamnogalacturonan acetylesterase (K4B1G1) and an expansin precursor (A7X331) (Table 3 in Ref [62]). Two of the GHs, belonging to families 17 (B5M9E5; beta-glucosidase 8 precursor) and 18 (K4CAY1; a predicted chitinase), showed increases among the largest measured in this study (21- and 5-fold, respectively), whereas the others increased markedly (between 2- and 5-fold). All these proteins are extracellular and participate in the hydrolysis and/or rearrangement of glycoside bonds in cell wall polysaccharides [77]. Five of the GHs belong to families 5 and 17, which are mainly endo-glucanases (CAZy description) and in conjunction with the two pectin-esterases, could participate in primary cell wall degradation. In line with this hypothesis, it has been described that Fe-deficiency causes a reduction in the xylem vessel size in leaves [78, 79], as well as changes in the lignification pattern in roots [80] and in the lignin/protein ratio in stem tissues [81]. Also, several GHs have been described as Fe-responsive in different sub-proteomes of Fe-deficient plants [49], with some increasing in abundance in the leaf apoplastic fluid [82]. Iron deficiency-induced modifications in the primary cell wall may affect sap flow and composition by altering permeability, although it has also been speculated that the increases in abundance of GHs may lead to an extra C supply to complement the low photosynthetic rates of Fe deficient plants [83]. Additionally, four GHs belonging to families 18, 19 and 20 are N-acetyl-hexosaminidases, mainly involved in N-glycan degradation, and therefore their increases may indicate a decrease in N-glycosylation, which is assumed to be a major post-translational modification of secreted proteins.

Conversely, Mn deficiency led to a down regulation of primary cell wall metabolism. Thirteen polysaccharide-related proteins decreased in abundance, with nine of them being GHs, two being pectic-modifying enzymes and two more being related to rhamnogalacturonan

metabolism (a lyase and an acetylesterase) (Table 4 in Ref [62]). Among the GHs decreasing in abundance, two belong to GH families 10 and 17 (xylanases and endoglucanases) involved in cellulose and xylan degradation whereas three more belong to GH 19, 20 and 35 (N-acetyl-glucosaminidase, N-acetyl-galactosaminidase, and β-galactosidase) which hydrolyze C-N bonds. These decreases suggest that processes involving cell wall and N-glycan degradation may be reduced in the xylem sap of Mn-deficient plants, conversely to what was observed in the case of Fe deficiency. Likewise, the decreases in two pectin esterases and in three proteins affecting galacturonate residues (a rhamnogalacturonate lyase, the polygalacturonase GH-28 and a rhamnogalacturonate acetylesterase), which are very abundant in pectic polysaccharides, support that primary cell wall degradation is reduced upon Mn deficiency. Overall, the changes induced by Mn-deficiency could lead to modifications in the rigidity of the primary cell wall, following the opposite direction than those observed with Fe deficiency.

4.4. Several xylem signaling pathways seem to play a role in the response to nutrient deficiencies

Data suggest that a CLE (CLAVATA3/EMBRYO SURROUNDING REGION-RELATED; CLV3/ESR-related) signaling pathway could be elicited in the xylem in response of Fe deficiency. The largest increases in abundance with Fe-deficiency were measured in two leucine rich repeat-receptor like kinases (LRR-RLK), K4D0Y5 and K4B2Y3 (57- and 33-fold increases, respectively), with K4B2Y3 showing one of the largest decreases in abundance (> 99%) upon Mn deficiency. The function of K4B2Y3 is unknown, but it is likely that this LRR-RLK is involved in a signaling pathway induced under Fe deficiency but repressed under Mn-deficient conditions. An antagonistic regulation of Mn and Fe acquisition has been recently proposed to occur in a genomics and proteomics study on whole *Arabidopsis* roots [52]. The *Arabidopsis* orthologue of K4D0Y5 (AtSKM1, At2g25790) participates in the CLE45 signaling pathway [84,

85]. CLE45 mitigates heat stress by binding with SKM1/SKM2 to sustain pollen growth under high temperatures [84]. Members of the CLE peptide family are xylem borne, composed of 12 or 13 amino acids and play crucial roles in xylem developmental processes [86-90]. Furthermore, members of the CLE family are involved in N and P stress signaling pathways that regulate plant growth and development [91]. Therefore, it is tempting to speculate that a xylem CLE signaling pathway is also involved in the response to Fe deficiency via K4D0Y5, and that this pathway may regulate Fe-induced changes in xylem growth processes.

Data also suggest that a lipid-based signaling system exists in the xylem sap that is tuned differently in the Fe and Mn deficiencies. In the phloem, lipids have been proposed as long-distance signals in response to abiotic stress in a mechanism that involves a putative GDSL-motif lipase, PIG-P-like protein, with a possible receptor-like function, and a lipid transfer protein [92, 93]. Proteins involved in lipid metabolism were affected by both nutrient deficiencies (five and six proteins in Fe and Mn deficiency, respectively). The second largest increase in Fe deficient xylem sap was measured in a GDSL-motif lipase (K4DD79; 47-fold). The exact role that this lipase plays in the Fe deficiency response is not clear. However, the presence of four more proteins related to lipid metabolism (two increasing and two decreasing), and especially the 3-fold increase of a lipid transfer protein (K4BFV4) could support the existence of a lipid-based signaling system in the xylem sap [2]. Interestingly, upon Mn shortage, significant decreases were measured in all six proteins related to lipid metabolism, including a GDSL motif lipase and two lipid transfer proteins. The fact that these proteins decreased upon Mn-deficiency could indicate that this signaling pathway is repressed under Mn stress, different to what occurs with Fe deficiency. However, one of them, a phosphatidylinositol-specific phospholipase C (PI-PLC) domain-containing protein (K4B315) decreased in both treatments

(Table 4). PI-PLCs often play important roles in various signaling cascades [94, 95] and therefore its decrease might indicate a common regulatory control point occurring in both deficiencies.

It is also worth mentioning that signaling-related fasciclin-like arabinogalactan proteins decreased in abundance in the xylem sap of plants affected by both nutrient deficiencies, including three in Mn-deficient (FLA-2, 11- and 12-like) and one in Fe-deficient (FLA-9-like) xylem sap. The FLA-11- and 12-like proteins belong to a subset of FLAs (groupA) that appear to contribute to the biomechanical properties (strength and elasticity) of stems through their impact on the synthesis and architecture of the secondary cell wall [31, 96].

Iron and Mn deficiencies also affect phosphorylation and glycosylation processes, as judged by changes in PAPs abundances, with modifications generally following an opposite pattern. Upon Fe deficiency, four purple acid phosphatases (PAPs) showed abundance increases ranging between 3 and 9-fold. These increases may account for changes in the phosphorylation status of the xylem sap, in line with the proposed existence of an extracellular phosphorylation network [97]. It is generally thought that a main role for PAPs is to provide P to overcome P starvation conditions [98, 99], but some PAPs are extracellular and can also dephosphorylate GHs, thus modulating their activities in the cell walls [100]. Given that PAPs are Fe-containing proteins, their increases in abundance upon Fe starvation denote important roles. Having this in mind, and since a human PAP can act as an Fe transporter in combination with ascorbate [101], it is tempting to speculate that these proteins may also somehow participate in the transport of Fe in the xylem sap. In Mn-deficient xylem sap, considerable decreases (60-90%) were measured in the PAPs abundances, opposite to what was observed upon Fe deficiency. This supports that in Mn limiting conditions proteins would likely remain phosphorylated when compared to control

and/or Fe-deficient xylem sap, thus revealing a different tuning of phosphorylation in Fe and Mn stresses. A similar situation was observed for N-glycosylation, since, as commented in Section 4.3, GHs hydrolyzing C-N bonds increased in abundance in xylem sap of Fe deficient plants but decreased in Mn-deficient ones.

4.5. Synthesis of proteins associated to the xylem sap is elicited by Fe deficiency and decreased by Mn deficiency

Interestingly, four structural components of the ribosome increased in abundance in Fe- deficient xylem sap whereas four decreased in Mn-deficient xylem sap, one of them showing one of the largest decreases observed (89%). Since most of these proteins were classified as NCS, this suggests that Fe deficiency causes an increase in the abundance of ribosomes located in cells having a close proximity to the xylem vessels, therefore being easily leaked upon cell rupture during xylem sampling. This is in line first with the large number of proteins increasing (60%) and decreasing (82%) in abundance in Fe and Mn deficient conditions, respectively, which would imply that *de novo* synthesis of proteins is not needed in Mn deficiency, and second with the opposite changes observed in certain proteases that can be involved in protein maturation (Table 4).

Conflict of interest

Authors declare no conflict of interest.

Acknowledgements

Supported by the Spanish Ministry of Economy and Competitiveness (MINECO; projects AGL2013-42175-R and AGL2016-75226-R, co-financed with FEDER), and the Aragón Government (Group A03). Research conducted in Iwate University was in part supported by Grants-in-Aid for Scientific Research (#24-7373, #22120003, and #24370018) from the Japan Society for the Promotion of Science. E.G.-C. was supported by a JAE Pre-CSIC contract and L. C.-L was supported by a FPI-MINECO contract. Authors thank Bruno Contreras-Moreira for his invaluable help with the data repository.

References

[1] D.B. Fisher. Long-distance transport in: B. Buchanan, W. Gruissem, R. Jones (Eds.) Biochemistry and Molecular Biology of Plants American Society of Plant Physiologists (2000) pp. 729-784.

[2] P. Carella, D.C. Wilson, C.J. Kempthorne, R.K. Cameron. Vascular sap proteomics: Providing insight into long-distance signaling during stress. Front. Plant Sci. 7 (2016).

[3] R.E. Dickson. Xylem translocation of amino-acids from roots to shoots in cottonwood plants. Can. J. Forest Res. 9 (1979) 374-378.

[4] P. Escher, M. Eiblmeier, I. Hetzger, H. Rennenberg. Seasonal and spatial variation of carbohydrates in mistletoes (*Viscum album*) and the xylem sap of its hosts (*Populus x euamericana and Abies alba*). Physiol. Plant. 120 (2004) 212-219.

[5] R. Friedman, N. Levin, A. Altman. Presence and identification of polyamines in xylem and phloem exudates of plants. Plant Physiol. 82 (1986) 1154-1157.

[6] A.F. López-Millán, F. Morales, A. Abadía, J. Abadía. Effects of iron deficiency on the composition of the leaf apoplastic fluid and xylem sap in Sugar Beet. Implications for iron and carbon transport. Plant Physiol. 124 (2000) 873-884.

[7] J. Rodríguez-Celma, L. Ceballos-Laita, M.A. Grusak, J. Abadía, A.F. López-Millán. Plant fluid proteomics: delving into the xylem sap, phloem sap and apoplastic fluid proteomes. Biochim. Biophys. Acta-Proteins and Proteomics 1864 (2016) 991–1002

[8] S. Satoh. Organic substances in xylem sap delivered to above-ground organs by the roots. J. Plant Res. 119 (2006) 179-187.

[9] S. Satoh, C. Iizuka, A. Kikuchi, N. Nakamura, T. Fujii. Proteins and carbohydrates in xylem sap from squash root. Plant Cell Physiol. 33 (1992) 841-847.

[10] S. Alvarez, J.Q.D. Goodger, E.L. Marsh, S. Chen, V.S. Asirvatham, D.P. Schachtman. Characterization of the maize xylem sap proteome. J. Proteome Res. 5 (2006) 963-972.

[11] H. Fukuda. Xylogenesis: initiation, progression, and cell death. Ann. Rev. Plant Physiol. Plant Mol. Biol. 47 (1996) 199-325.

[12] L. Ligat, E. Lauber, C. Albenne, H.S. Clemente, B. Valot, M. Zivy, R. Pont-Lezica, M. Arlat, E. Jamet. Analysis of the xylem sap proteome of *Brassica oleracea* reveals a high content in secreted proteins. Proteomics 11 (2011) 1798-1813.

[13] M.A. Djordjevic, M. Oakes, D.X. Li, C.H. Hwang, C.H. Hocart, P.M. Gresshoff. The *Glycine max* xylem sap and apoplast proteome. J. Proteome Res. 6 (2007) 3771-3779.

[14] S. Masuda, C. Sakuta, S. Satoh. cDNA cloning of a novel lectin-like xylem sap protein and its root-specific expression in cucumber. Plant Cell Physiol. 40 (1999) 1177-1181.

[15] C. Sakuta, S. Satoh. Vascular tissue-specific gene expression of xylem sap glycine-rich proteins in root and their localization in the walls of metaxylem vessels in cucumber. Plant Cell Physiol. 41 (2000) 627-638.

[16] A. Buhtz, A. Kolasa, K. Arlt, C. Walz, J. Kehr. Xylem sap protein composition is conserved among different plant species. Planta 219 (2004) 610-618.

[17] O. Pechanova, C.-Y. Hsu, J.P. Adams, T. Pechan, L. Vandervelde, J. Drnevich, S. Jawdy, A. Adeli, J.C. Suttle, A.M. Lawrence, T.J. Tschaplinski, A. Séguin, C. Yuceer. Apoplast proteome reveals that extracellular matrix contributes to multistress response in poplar. BMC Genomics 11 (2010) 1-22.

[18] M. Rep, H.L. Dekker, J.H. Vossen, A.D. de Boer, P.M. Houterman, C.G. de Koster, B.J.C. Cornelissen. A tomato xylem sap protein represents a new family of small cysteine-rich proteins with structural similarity to lipid transfer proteins. FEBS Lett. 534 (2003) 82-86.

[19] Y. Xia, H. Suzuki, J. Borevitz, J. Blount, Z. Guo, K. Patel, R.A. Dixon, C. Lamb. An extracellular aspartic protease functions in *Arabidopsis* disease resistance signaling. EMBO J. 23 (2004) 980-988.

[20] W.J. Lucas, A. Groover, R. Lichtenberger, K. Furuta, S.-R. Yadav, Y. Helariutta, X.-Q. He, H. Fukuda, J. Kang, S.M. Brady, J.W. Patrick, J. Sperry, A. Yoshida, A.F. López-Millán, M.A. Grusak, P. Kachroo. The plant vascular system: evolution, development and functions. J. Integr. Plant Biol. 55 (2013) 294-388.

[21] I.C. Dodd. Root-to-shoot signaling: assessing the roles of 'up' in the up and down world of long-distance signaling in plant. Plant and Soil 274 (2005) 251-270.

[22] M.E. Ghanem, A. Albacete, A.C. Smigocki, I. Frébort, H. Pospísilová, C. Martínez-Andújar, M. Acosta, J. Sánchez-Bravo, S. Lutts, I.C. Dodd, F. Pérez-Alfocea. Root-synthesized cytokinins improve shoot growth and fruit yield in salinized tomato (*Solanum lycopersicum L.*) plants. J. Exp. Bot. 62 (2011) 125-140.

[23] N. Hirose, K. Takei, T. Kuroha, T. Kamada-Nobusada, H. Hayashi, H. Sakakibara. Regulation of cytokinin biosynthesis, com-partmentalization and translocation. J. Exp. Bot. 59 (2008) 75-83.

[24] A.C. Martin, J. Del Pozo, J. Iglesias, V. Rubio, R. Solano, A. De La Pena, A. Leyva, J. Paz-Ares. Influence of cytokinins on the ex-pression of phosphate starvation responsive genes in *Arabidopsis*. Plant J. 24 (2000) 559-567.

[25] Y.S. Rahayu, P. Walch-Liu, G. Neumann, V. Römheld, N. von Wirén, F. Bangerth. Root-derived cytokinins as long-distance signalsfor NO^{-3}-induced stimulation of leaf growth. J. Exp. Bot. 56 (2005) 1143-1152.

[26] H. Rouached, A. Stefanovic, D. Secco, A.A. Bulak, E. Gout, R. Bligny, Y. Poirier. Uncoupling phosphate deficiency fromits major effects on growth and transcriptome via PHO1 expressionin *Arabidopsis*. Plant J. 65 (2011) 557-570.

[27] S. Ruffel, G. Krouk, D. Ristova, D. Shasha, K.D. Birnbaum, G.M. Coruzzi. Nitrogen economics of root foraging: Transitive closure of the nitrate-cytokinin relay and distinct systemic signaling for N supply vs. demand. Proc. Natl. Acad. Sci. U. S. A. 108 (2011) 18524-18529.

[28] K. Takei, T. Takahashi, T. Sugiyama, T. Yamaya, H. Sakakibara. Multiple routes communicating nitrogen availability from roots to shoots: A signal transduction pathway mediated by cytokinin. J. Exp. Bot. 53 (2002) 971-977.

[29] T. Aki, M. Shigyo, R. Nakano, T. Yoneyama, S. Yanagisawa. Nano scale proteomics revealed the presence of regulatory proteins including three FT-like proteins in phloem and xylem saps from rice. Plant Cell Physiol. 49 (2008) 767-790.

[30] H.B. Krishnan, S.S. Natarajan, J.O. Bennett, R.C. Sicher. Protein and metabolite composition of xylem sap from field-grown soybeans (*Glycine max*). Planta 233 (2011) 921-931.

[31] Z. Zhang, W. Xin, S. Wang, X. Zhang, H. Dai, R. Sun, T. Frazier, B. Zhang, Q. Wang. Xylem sap in cotton contains proteins that contribute to environmental stress response and cell wall development. Funct. Integr. Genomic. 15 (2015) 17-26.

[32] H. Marschner. Mineral nutrition of higher plants. Academic Press (1995).

[33] L.E. Williams, J.K. Pittman. Dissecting pathways involved in manganese homeostasis and stress in higher plant cells. Plant Cell Monographs 2010. p. 95-117.

[34] J. Nickelsen, B. Rengstl. Photosystem II assembly: From cyanobacteria to plants. Ann. Rev. Plant Biol. 2013. p. 609-635.

[35] A.L. Socha, M.L. Guerinot. Mn-euvering manganese: The role of transporter gene family members in manganese uptake and mobilization in plants. Front. Plant Sci. 5 (2014).

[36] J.K. Pittman. Managing the manganese: Molecular mechanisms of manganese transport and homeostasis. New Phytol. 167 (2005) 733-742.

[37] N. Msilini, M. Zaghdoudi, S. Govindachary, M. Lachaâl, Z. Ouerghi, R. Carpentier. Inhibition of photosynthetic oxygen evolution and electron transfer from the quinone acceptor QA - To QB by iron deficiency. Photosynth. Res. 107 (2011) 247-256.

[38] J.A. Raven, M.C.W. Evans, R.E. Korb. The role of trace metals in photosynthetic electron transport in O_2-evolving organisms. Photosynth. Res. 60 (1999) 111-149.

[39] S. Tottey, M.A. Block, M. Allen, T. Westergren, C. Albrieux, H.V. Scheller, S. Merchant, P.E. Jensen. *Arabidopsis* CHL27, located in both envelope and thylakoid membranes, is required for the synthesis of protochlorophyllide. Proc. Natl. Acad. Sci. U. S. A. 100 (2003) 16119-16124.

[40] J. Abadía, A. Álvarez-Fernández, A.D. Rombolá, M. Sanz, M. Tagliavini, A. Abadía. Technologies for the diagnosis and remediation of Fe deficiency. Soil Sci. Plant Nutr. 50 (2004) 965-971.

[41] J. Abadía, S. Vázquez, R. Rellán-Álvarez, H. El-Jendoubi, A. Abadía, A. Álvarez-Fernández, A.F. López-Millán. Towards a knowledge-based correction of iron chlorosis. Plant Physiol. Biochem. 49 (2011) 471-482.

[42] J.F. Briat, C. Dubos, F. Gaymard. Iron nutrition, biomass production, and plant product quality. Trends Plant Sci. 20 (2015) 33-40.

[43] W.Z. Jiang. Mn use efficiency in different wheat cultivars. Environ. Exp. Bot. 57 (2006) 41-50.

[44] P. Flis, L. Ouerdane, L. Grillet, C. Curie, S. Mari, R. Lobinski. Inventory of metal complexes circulating in plant fluids: a reliable method based on HPLC coupled with dual elemental and high-resolution molecular mass spectrometric detection. New Phytol. 211 (2016) 1129-1141.

[45] R. Rellán Álvarez, S. Andaluz, J. Rodríguez-Celma, G. Wohlgemuth, G. Zocchi, A. Álvarez-Fernández, O. Fiehn, A.F. López-Millán, J. Abadía. Changes in the proteomic and metabolic profiles of *Beta vulgaris* root tips in response to iron deficiency and resupply. BMC Plant Biol. 10 (2010) 1-15.

[46] M.C. White, A.M. Decker, R.L. Chaney. Metal complexation in xylem fluid: I. Chemical composition of tomato and soybean stem exudate. Plant Physiol. 67 (1981) 292-300.

[47] K. Kosová, P. Vítámvás, I.T. Prásil, J. Renaut. Plant proteome changes under abiotic stress - Contribution of proteomics studies to understanding plant stress response. J. Proteomics 74 (2011) 1301-1322.

[48] A.M. Timperio, M.G. Egidi, L. Zolla. Proteomics applied on plant abiotic stresses: role of heat shock proteins (HSP). J. Proteomics 71 (2008) 391-411.

[49] A.F. López-Millán, M.A. Grusak, A. Abadía, J. Abadía. Iron deficiency in plants: an insight from proteomic approaches. Front. Plant Sci. 4 (2013) 254.

[50] H.J. Mai, P. Bauer. From the proteomic point of view: Integration of adaptive changes to iron deficiency in plants. Curr. Plant Biol. 5 (2016) 45-56.

[51] M.M. Fecht-Christoffers, H.-P. Braun, C. Lemaitre-Guillier, A. VanDorsselaer, W.J. Horst. Effect of manganese toxicity on the proteome of the leaf apoplast in cowpea. Plant Physiol. 133 (2003) 1935-1946.

[52] J. Rodríguez-Celma, Y.H. Tsai, T.N. Wen, Y.C. Wu, C. Curie, W. Schmidt. Systems-wide analysis of manganese deficiency-induced changes in gene activity of *Arabidopsis* roots. Sci. Rep. 6 (2016) 35846.

[53] N. Fernandez-García, M. Hernandez, J. Casado-Vela, R. Bru, F. Elortza, P. Hedden, E. Olmos. Changes to the proteome and targeted metabolites of xylem sap in *Brassica oleracea* in response to salt stress. Plant Cell Environ. 34 (2011) 821-836.

[54] C. Liao, R. Liu, F. Zhang, C. Li, X. Li. Nitrogen under- and oversupply induces distinct protein responses in maize xylem sap. Journal of Integrative Plant Biol. 54 (2012) 374-387.

[55] Z. Zhang, M. Chao, S. Wang, J. Bu, J. Tang, F. Li. Proteome quantification of cotton xylem sap suggests the mechanisms of potassium deficiency-induced changes in plant resistance to environmental stresses. Sci. Rep. 6 (2016) 21060.

[56] D. Takahashi, B. Li, T. Nakayama, Y. Kawamura, M. Uemura. Shotgun proteomics of plant plasma membrane and microdomain proteins using nano-LC-MS/MS in J.V.J Novo, S. Komatsu, W. Wechwerth, S. Wienkoopeds (Eds.) Plant proteomics: Methods and protocols (2014) pp. 481-498.

[57] E. Gutierrez-Carbonell, D. Takahashi, S. Lüthje, J.A. González-Reyes, S. Mongrand, B. Contreras-Moreira, A. Abadía, M. Uemura, J. Abadía, A.F. López-Millán. A shotgun proteomic approach reveals that Fe deficiency causes marked changes in the protein profiles of plasma membrane and detergent-resistant microdomain preparations from *Beta vulgaris* roots. J. Proteome Res. 15 (2016) 2510-2524.

[58] D. Takahashi, Y. Kawamura, M. Uemura. Changes of detergent-resistant plasma membrane proteins in oat and rye during cold acclimation: association with differential freezing tolerance. J. Proteome Res. 12 (2013) 4998-5011.

[59] O. Emanuelsson, S. Brunak, G. VonHeijne, H. Nielsen. Locating proteins in the cellusing TargetP, SignalP and related tools. Nat. Protoc. 2 (2007) 953-971.

[60] J. Bendtsen, L. Kiemer, A. Fausboll, S. Brunak. Non-classical protein secretion in bacteria. BMC Microbiol. 5 (2005) 58.

[61] J.D. Bendtsen, L.J. Jensen, N. Blom, G. VonHeijne, S. Brunak. Feature-based prediction of non-classical and leader less protein secretion. Prot. Eng. Des. Sel. 17 (2004) 349-356.

[62] L. Ceballos-Laita, E. Gutierrez-Carbonell, D. Takahashi, A. Abadía, M. Uemura, J. Abadía, A.F. López-Millán. Data on xylem sap from Mn- and Fe-deficient tomato plants. J. Proteomics, Data in Brief, *submitted*.

[63] Z. Li, D. Phillip, B. Neuhäuser, W.X. Schulze, U. Ludewig. Protein dynamics in young maize root hairs in response to macro- and micronutrient deprivation. J. Proteome Res. 14 (2015) 3362-3371.

[64] S.M. Zargar, M. Fujiwara, S. Inaba, M. Kobayashi. Correlation analysis of proteins responsive to Zn, Mn, or Fe deficiency in *Arabidopsis* roots based on iTRAQ analysis. Plant Cell Rep. 34 (2015) 157-166.

[65] P. Lan, W. Li, T.-N. Wen, J.-Y. Shiau, Y.-C. Wu, W. Lin, W. Schmidt. iTRAQ protein profile analysis of *Arabidopsis* roots reveals new aspects critical for iron homeostasis. Plant Physiol. 155 (2011) 821-834.

[66] B.T. Zaharieva, J. Abadía. Iron deficiency enhances the levels of ascorbate, glutathione, and related enzymes in Sugar beet roots. Protoplasma 221 (2003) 269-275.

[67] A. Schaller. A cut above the rest: the regulatory function of plant proteases. Planta 220 (2004) 183-197.

[68] F. Fernández-Pérez, F. Pomar, M.A. Pedreño, E. Novo-Uzal. The suppression of AtPrx52 affects fibers but not xylem lignification in *Arabidopsis* by altering the proportion of syringyl units. Physiol. Plant. 154 (2015) 395-406.

[69] J. Shigeto, M. Nagano, K. Fujita, Y. Tsutsumi. Catalytic profile of *Arabidopsis* peroxidases, AtPrx-2, 25 and 71, contributing to stem lignification. PLoS ONE 9 (2014).

[70] J. Shigeto, Y. Tsutsumi. Diverse functions and reactions of class III peroxidases. New Phytol. 209 (2016) 1395-1402.

[71] C. Chassot, C. Nawrath, J.-P. Métraux. Cuticular defects lead to full immunity to a major plant pathogen. Plant J. 49 (2007) 972-980.

[72] C. Carter, R.W. Thornburg. Tobacco Nectarin I: purification and characterization as a germin-like, manganese superoxide dismutase implicated in the defense of floral reproductive tissues. J. Biol. Chem. 275 (2000) 36726-36733.

[73] P.V. Turlapati, K.W. Kim, L.B. Davin, N.G. Lewis. The laccase multigene family in *Arabidopsis thaliana:* towards addressing the mystery of their gene function(s). Planta 233 (2011) 439-470.

[74] M. Ferretti, T. Destro, S.C.E. Tosatto, N. La Rocca, N. Rascio, A. Masi. Gamma-glutamyl transferase in the cell wall participates in extracellular glutathione salvage from the root apoplast. New Phytol. 181 (2009) 115-126.

[75] N. Ohkama-Ohtsu, S. Radwan, A. Peterson, P. Zhao, A.F. Badr, C. Xiang, D.J. Oliver. Characterization of the extracellular γ-glutamyl transpeptidases, GGT1 and GGT2, in *Arabidopsis.* Plant J. 49 (2007) 865-877.

[76] T. Maruta, Y. Ichikawa, T. Mieda, T. Takeda, M. Tamoi, Y. Yabuta, T. Ishikawa, S. Shigeoka. The contribution of *Arabidopsis* homologs of L-gulono-1,4-lactone oxidase to the biosynthesis of ascorbic acid. Biosci. Biotech. Biochem. 74 (2010) 1494-1497.

[77] Z. Minic. Physiological roles of plant glycoside hydrolases. Planta 227 (2008) 723-740.

[78] T. Eichert, J.J. Peguero-Pina, E. Gil-Pelegrín, A. Heredia, V. Fernández. Effects of iron chlorosis and iron resupply on leaf xylem architecture, waterrelations, gas exchange and stomatal performance offield-grown peach (*Prunus persica*). Physiol. Plant. 138 (2010) 48-59.

[79] V. Fernández, T. Eichert, V. Del Río, G. López-Casado, J.A. Heredia-Guerrero, A. Abadía, A. Heredia, J. Abadía. Leaf structural changes associated with iron deficiency chlorosis in field-grown pear and peach: Physiological implications. Plant and Soil 311 (2008) 161-172.

[80] S. Donnini, A. Castagna, A. Ranieri, G.J. Zocchi. Differential responses in pear and quince genotypes induced by Fe deficiency and bicarbonate. Plant Physiol. 166 (2009) 1181-1193.

[81] J. Rodríguez-Celma, G. Lattanzio, D. Villarroya, E. Gutierrez-Carbonell, L. Ceballos-Laita, J. Rencoret, A. Gutiérrez, J.C. Del Río, M.A. Grusak, A. Abadía, J. Abadía, A.F. López-Millán. Effects of Fe deficiency on the protein profiles and lignin composition of stem tissues from *Medicago truncatula* in absence or presence of calcium carbonate. J. Proteomics 140 (2016) 1-12.

[82] L. Ceballos-Laita, E. Gutierrez-Carbonell, S.V. Lattanzio, G. , B. Contreras-Moreira, A. Abadía, J. Abadía, A.F. López-Millán. Protein profile of *Beta vulgaris* leaf apoplastic fluid and changes induced by Fe deficiency and Fe resupply. Front. Plant Sci. 6 (2015) 145.

[83] S. Donnini, B. Prinsi, A.S. Negri, G. Vigani, L. Espen, G. Zocchi. Proteomic characterization of iron deficiency responses in *Cucumis sativus* L. roots. . BMC Plant Biol. 10 (2010) 268.

[84] S. Endo, H. Shinohara, Y. Matsubayashi, H. Fukuda. A novel pollen-pistil interaction conferring high-temperature tolerance during reproduction via CLE45 signaling. Curr. Biol. 23 (2013) 1670-1676.

[85] Y.H. Kang, C.S. Hardtke. *Arabidopsis* MAKR5 is a positive effector of BAM3-dependent CLE45 signaling. EMBO Rep. 17 (2016) 1145-1154.

[86] Y. Hirakawa, Y. Kondo, H. Fukuda. TDIF peptide signaling regulates vascular stem cell proliferation via the WOX4 homeobox gene in *Arabidopsis*. Plant Cell 22 (2010) 2618-2629.

[87] Y. Hirakawa, H. Shinohara, Y. Kondo, A. Inoue, I. Nakanomyo, M. Ogawa, S. Sawa, K. Ohashi-Ito, Y. Matsubayashi, H. Fukuda. Non-cell-autonomous control of vascular stem cell fate by a CLE peptide/receptor system. Proc. Natl. Acad. Sci. 105 (2008) 15208-15213.

[88] Y. Ito, I. Nakanomyo, H. Motose, K. Iwamoto, S. Sawa, N. Dohmae, H. Fukuda. Dodeca-CLE peptides as suppressors of plant stem cell differentiation. Science 313 (2006) 842-845.

[89] K. Ohyama, H. Shinohara, M. Ogawa-Ohnishi, Y. Matsubayashi. A glycopeptide regulating stem cell fate in *Arabidopsis thaliana*. Nat. Chem. Biol. 5 (2009) 578-580.

[90] Y. Stahl, R.H. Wink, G.C. Ingram, R. Simon. A signaling module controlling the stem cell niche in *Arabidopsis* root meristems. Curr. Biol. 19 (2009) 909-914.

[91] G. Wang, G. Zhang, M. Wu. CLE peptide signaling and crosstalk with phytohormones and environmental stimuli. Front. Plant Sci. 6 (2015) 1211.

[92] A.M. Barbaglia, B. Tamot, V. Greve, S. Hoffmann-Benning. Phloem proteomics reveals new lipid-binding proteins with a putative role in lipid-mediated signaling. Front. Plant Sci. 7 (2016) 563.

[93] U.F. Benning, B. Tamot, B.S. Guelette, S. Hoffmann-Benning. New aspects of phloem-mediated long-distance lipid signaling in plants. Front. Plant Sci. 3 (2012) 53.

[94] S.N. Hicks, M.R. Jezyk, S. Gershburg, J.P. Seifert, T.K. Harden, J. Sondek. General and versatile autoinhibition of PLC isozymes. Mol. Cell 31 (2008) 383-394.

[95] E. Meldrum, P.J. Parker, A. Carozzi. The PtdIns-PLC superfamily and signal transduction. Biochim. Biophys. Acta 1092 (1991) 49-71.

[96] C.P. MacMillan, S.D. Mansfield, Z.H. Stachurski, R. Evans, S.G. Southerton. Fasciclin-like arabinogalactan proteins: specialization for stem biomechanics and cell wall architecture in *Arabidopsis* and Eucalyptus. Plant J. 62 (2010) 689-703.

[97] B.K. Ndimba, S. Chivasa, J.M. Hamilton, W.J. Simon, A.R. Slabas. Proteomic analysis of changes in the extracellular matrix of *Arabidopsis* cell suspension cultures induced by fungal elicitors. Proteomics 3 (2003) 1047-1059.

[98] H.A. Del Vecchio, S. Ying, J. Park, V.L. Knowles, S. Kanno, K. Tanoi, Y.-M. She, W.C. Plaxton. The cell wall-targeted purple acid phosphatase AtPAP25 is critical for acclimation of *Arabidopsis thaliana* to nutritional phosphorus deprivation. Plant J. 80 (2014) 569-581.

[99] W.D. Robinson, I. Carson, S. Ying, K. Ellis, W.C. Plaxton. Eliminating the purple acid phosphatase AtPAP26 in *Arabidopsis thaliana* delays leaf senescence and impairs phosphorus remobilization. New Phytol. 196 (2012) 1024-1029.

[100] R. Kaida, S. Serada, N. Norioka, S. Norioka, et al. Potential role for purple acid phosphatase in the dephosphorylation of wall proteins in tobacco cells. Plant Physiol. 153 (2010) 603-610.

[101] P.R. Nuttleman, R.M. Roberts. Transfer of iron from uteroferrin (purple acid phosphatase) to transferrin related to acid phosphatase activity. J. Biol. Chem. 265 (1990) 12192-12199.

Tables

Table 1- Xylem sap properties and leaf chlorophyll estimation. Xylem sap exudation rates (ml plant^{-1} h^{-1}), protein extraction yields (ng protein µL^{-1} xylem sap) and metal concentrations (µM), and leaf SPAD values from control, Fe-deficient and Mn-deficient plants. Values are means ± SD (n = 6). Different letters within the same row indicate statistically significant differences (Student's t- test, $p \leq 0.05$).

Xylem sap properties	**Control**	**- Fe**	**- Mn**
Exudation rates (mL plant^{-1} h^{-1})	0.8 ± 0.1 a	0.8 ± 0.2 a	1.1 ± 0.3 b
Protein extraction yield (ng protein µL^{-1} xylem sap)	9.0 ± 3.4 b	6.9 ± 1.7 b	4.2 ± 2.5 a
[Fe]	47.8 ± 12.5 c	15.5 ± 6.9 a	26.6 ± 4.2 b
[Mn]	6.5 ± 0.8 b	7.7 ± 3.2 b	0.7 ± 0.6 a
[Cu]	3.6 ± 0.8 a	3.6 ± 1.3 a	3.0 ± 0.5 a
[Zn]	9.5 ± 1.3 a	9.3 ± 4.7 a	7.0 ± 0.6 a
Leaf SPAD values	42.4 ± 4.1 c	13.6 ± 3.3 a	29.6 ± 4.9 b

Table 2- Proteins showing the large changes in abundance (fold > 5 or < 0.2) among the secretory proteins affected by Fe-deficiency (ANOVA, $p \leq 0.05$ and fold ≥ 2 or ≤ 0.5). Accession indicates protein UniProt database entry. Pep_c/Pep_q indicates the number of peptides assigned to a protein and number of peptides used for quantification. Abundance changes (Fold –Fe/control) were calculated by dividing the relative mean abundances in Fe-deficient (mean -Fe) by that of control samples (mean control). SecretomeP column indicates results from subcellular classification as classical (CS) and non-classical secretory (NCS) protein. Detailed information about functional classification, subcellular localization, identification and quantification is given in Table 3 in Ref [62].

Accession	Pep_c/Pep_q	Mean Control	Mean -Fe	Fold -Fe/Control	Description	SecretomeP
				Proteolysis		
K4B033	12 / 12	2448669	13965079	5.70	predicted protein aspartic protease in guard cell 2-like (MEROPS A1)	CS
O82777	10 / 6	21221	140320	6.61	subtilisin-like protease Sbt3 (MEROPS S8)	NCS
K4CYB7	4 / 4	5979	59119	9.89	predicted protein aspartic protease in guard cell 1 (MEROPS A1)	CS
K4C8U3	11 / 10	1400622	19995731	14.28	predicted miraculin-like (MEROPS inhibitor I3, clan IC)	CS
K4AXP3	4 / 4	6188	128020	20.69	predicted basic 7S globulin-like (MEROPS A1)	CS
				Polysaccharide metabolism		
K4CAY1	6 / 6	150109	769252	5.12	predicted chitinase (GH-18)	CS
B5M9E5	3 / 3	2681	56597	21.11	beta-glucosidase 8 precursor (GH-17)	CS
				Oxidoreductases		
K4D7T6	10 / 9	535353	93758	0.18	predicted peroxidase 44-like isoform 1	CS

					(AtPER44-like)	
K4C5I8	5 / 3	12142	88166	7.26	predicted peroxidase 4-like (AtPER52-like)	CS
K4BFP3	3 / 2	7041	82696	11.75	predicted peroxidase 72-like (AtPER72-like)	CS
				Lipid metabolism		
K4DD79	4 / 4	454	21484	47.32	predicted GDSL esterase/lipase At1g28590-like	CS
				Signaling/regulation		
K4B2Y3	3 / 3	2622	86415	32.96	probable LRR receptor-like serine/threonine-protein kinase	CS
K4D0Y5	19 / 18	51184	2924595	57.14	LRR receptor-like protein kinase	CS
				Phosphatases		
K4C6W9	3 / 3	9599	75298	7.84	similar to predicted acid phosphatase 1-like	CS
K4CPW9	16 / 14	227820	1945258	8.54	predicted probable inactive purple acid phosphatase 1	CS
				Unassigned/Unknown		
K4CP48	6 / 2	2243	25827	11.51	similar to conglutin (*Medicago truncatula*)	CS
K4BDM8	2 / 2	22624	119293	5.27	uncharacterized protein	CS

Table 3- Proteins showing the large changes in abundance (fold > 5 or < 0.2) among the secretory proteins affected by Mn-deficiency (ANOVA, $p \leq 0.05$ and fold ≥ 2 or ≤ 0.5). Accession indicates protein UniProt database entry. Pep_c/Pep_q indicates the number of peptides assigned to a protein and number of peptides used for quantification. Abundance changes (Fold –Mn/control) calculated by dividing the relative mean abundances in Mn-deficient (mean -Mn) by that of control samples (mean control). SecretomeP column indicates results from subcellular classification as classical (CS) and non-classical secretory (NCS) protein. Detailed information about functional classification, subcellular localization, identification and quantification is given in Table 4 in Ref [62].

Accession	Pep_c/Pep_q	Mean Control	Mean -Mn	Fold -Mn/Control	Description	SecretomeP
			Protein metabolism (Proteolysis and protein synthesis)			
K4D3L8	10 / 8	429869	57130	0.13	predicted subtilisin-like protease-like (MEROPS S8)	CS
K4CUW3	2 / 2	25208	2787	0.11	similar to 60S ribosomal protein L17	CS
			Signaling/regulation			
K4B2Y3	3 / 3	2622	21	0.01	probable LRR receptor-like Ser/Thr- kinase	CS
			ATP Hydrolysis coupled to proton transport			
Q2MIB5	6 / 6	20384	142383	6.99	similar to ATP synthase CF1 alpha chain	NCS
			Phosphatases			
K4D9N7	4 / 4	95980	11757	0.12	native purple acid phosphatase 29-like	CS
K4DC68	3 / 3	31485	4507	0.14	predicted bifunctional purple acid phosphatase 26	CS
			Unassigned/Unknown			
G3XKQ7	2 / 2	4416	56	0.01	endonuclease 1	CS

K4CGQ4	4 / 4	300874	43580	0.14	predicted uncharacterized protein LOC101247939	CS
K4D0G7	2 / 2	17572	2780	0.16	predicted uncharacterized protein At4g06744-like	CS
K4B0S2	4 / 4	4651	33934	7.30	similar to NAD(P)-binding Rossmann-fold protein	NCS
K4CHI8	2 / 2	851	11666	13.71	uncharacterized protein	CS

Table 4- List of the 24 secretory proteins (identified and quantified with at least two unique peptides) affected by both deficiencies (ANOVA, $p \leq 0.05$ and fold ≥ 2 or ≤ 0.5). Accession (UniProt identifiers) and protein description are shown in the first two columns, fold changes induced by Fe (-Fe/C) and Mn (-Mn/C) deficiencies were calculated by dividing the relative mean abundances in deficient by that of control samples. SecretomeP column indicates results from subcellular classification as classical (CS) and non-classical secretory (NCS) protein. Detailed information about functional classification, subcellular localization, identification and quantification is given in Tables 3 and 4 in Ref [62].

Accession	Description	-Fe/C	-Mn/C	SecretomeP
K4D7T6	predicted peroxidase AtPER44-like isoform 1 (AtPER44-like)	0.18	0.21	CS
K4BTH7	predicted peroxidase AtPER12-like	0.32	0.41	CS
K4C1C0	predicted cationic peroxidase 1 (AtPER52-like)	0.35	0.43	CS
K4ATR4	predicted serine carboxypeptidase-like 45. (MEROPS S10)	0.22	0.30	CS
K4D3L8	predicted subtilisin-like protease (MEROPS S8)	0.36	0.13	CS
K4C895	predicted protein aspartic protease in guard cell 1 (MEROPS A1)	0.48	0.43	NCS
K4B315	predicted PI-PLC X domain-containing protein; At5g67130-like (Phosphatidylinositol-specific phospholipase C)	0.37	0.29	CS
K4CGQ4	predicted uncharacterized protein LOC101247939	0.42	0.14	CS
K4CG62	similar to ribosomal protein L11-like (*Nicotiana tabacum*)	2.01	0.35	NCS
K4BA70	similar to 40S ribosomal protein S15-like (*Solanum tuberosum*)	2.07	0.31	NCS
K4CUW3	similar to 60S ribosomal protein L17 (*Arabidopsis thaliana*)	2.49	0.11	CS
B5M9E5	beta-glucosidase 8 precursor (GH-17)	21.11	0.28	CS
K4D4J5	predicted cell wall / vacuolar inhibitor of fructosidase 2-like (Pectinesterase_inhib_dom.)	3.09	0.47	CS
K4B1G1	rhamnogalacturonan acetylesterase-At4g34215-like (SGNH-hydro)	3.22	0.44	CS
Q6RHX9	xyloglucan endotransglucosylase-hydrolase XTH6 precursor (GH-16)	3.59	0.34	CS

K4CBX5	predicted probable inactive purple acid phosphatase 27	2.74	0.42	CS
K4CPW9	predicted probable inactive purple acid phosphatase 1	8.54	0.41	CS
K4DC68	predicted bifunctional purple acid phosphatase 26	3.20	0.14	CS
K4DGL5	predicted protein aspartic protease in guard cell 1 (MEROPS A1)	3.89	0.32	CS
K4CYB7	predicted protein aspartic protease in guard cell 1 (MEROPS A1)	9.89	0.24	CS
K4B2Y3	probable LRR receptor-like Ser/Thr- kinase	32.96	0.01	CS
G3XKQ7	endonuclease 1	2.57	0.01	CS
K4B1G7	predicted nectarin-1 (MnSOD-like)	3.30	0.29	NCS
K4BE45	predicted uncharacterized protein LOC101253159	3.64	0.38	CS

Figure legends

Figure 1- Effect of Fe-deficiency on the xylem protein profile as revealed by label-free shotgun analyses. Volcano scatter plot (A) showing the 643 identified and quantified proteins (peptides assigned to a protein and used for quantification ≥ 2) where proteins unaffected by Fe deficiency are depicted in grey and proteins changing as a result of Fe deficiency (ANOVA, $p \leq 0.05$) are depicted green (decreasing) or red (increasing). Light colors are used for those proteins meeting only the statistical threshold (ANOVA, $p \leq 0.05$) and bright colors where used when the statistical and biological (fold change ≤ 0.5 or ≥ 2) thresholds were met. The size of the dots is proportional to the fold changes. Pie chart depicting subcellular classification (NS: non-secretory, CS: classical secretory and NCS: non-classical secretory) as revealed by SignalP and SecretomeP prediction tools of proteins showing decreased (B) and increased (C) abundances. Functional classification based on GO biological process and domain annotations of secretory proteins showing decreased (D) and increased (E) abundances as a result of Fe deficiency.

Figure 2- Effect of Mn-deficiency on the xylem protein profile as revealed by label-free shotgun analyses. Volcano scatter plot (A) showing the 643 identified and quantified proteins (peptides assigned to a protein and used for quantification ≥ 2) where proteins unaffected by Mn deficiency are depicted in grey and proteins changing as a result of Mn deficiency (ANOVA, $p \leq 0.05$) are depicted green (decreasing) or red (increasing). Light colors are used for those proteins meeting only the statistical threshold (ANOVA, $p \leq 0.05$) and bright colors where used when the statistical and biological (fold change ≤ 0.5 or ≥ 2) thresholds were met. The size of the dots is proportional to the fold changes. Pie chart depicting subcellular classification (NS: non-secretory, CS: classical secretory

and NCS: non-classical secretory) as revealed by SignalP and SecretomeP prediction tools of proteins showing decreased (B) and increased (C) abundances. Functional classification based on GO biological process and domain annotations of secretory proteins showing decreased (D) and increased (E) abundances as a result of Fe deficiency.

Figure 3- A) Venn diagram comparing the number of secretory proteins changing as a result of Fe and Mn deficiency ($p \leq 0.05$, number of peptides for identification and quantification ≥ 2 and fold ≤ 0.5 or ≥ 2). B) Functional classification of all secretory proteins showing changes in Fe and Mn deficiencies. Proteins showing significant changes in both comparisons ($p \leq 0.05$), identified and quantified with at least two peptides, and above the threshold level (fold change ≥ 2 or ≤ 0.5) were classified according to their functions. Green and orange bars indicate number of proteins decreasing and increasing in relative abundance in Fe-deficiency and Mn-deficiency, respectively. C) Functional classification of the 24 common secretory proteins showing changes in both treatments. Proteins showing significant changes in both comparisons ($p \leq 0.05$), identified and quantified with at least two peptides, and above the threshold level (fold change ≥ 2 or ≤ 0.5) were classified according to their functions. Green and orange bars indicate number of proteins decreasing and increasing in relative abundance in Fe-deficiency and Mn-deficiency, respectively.

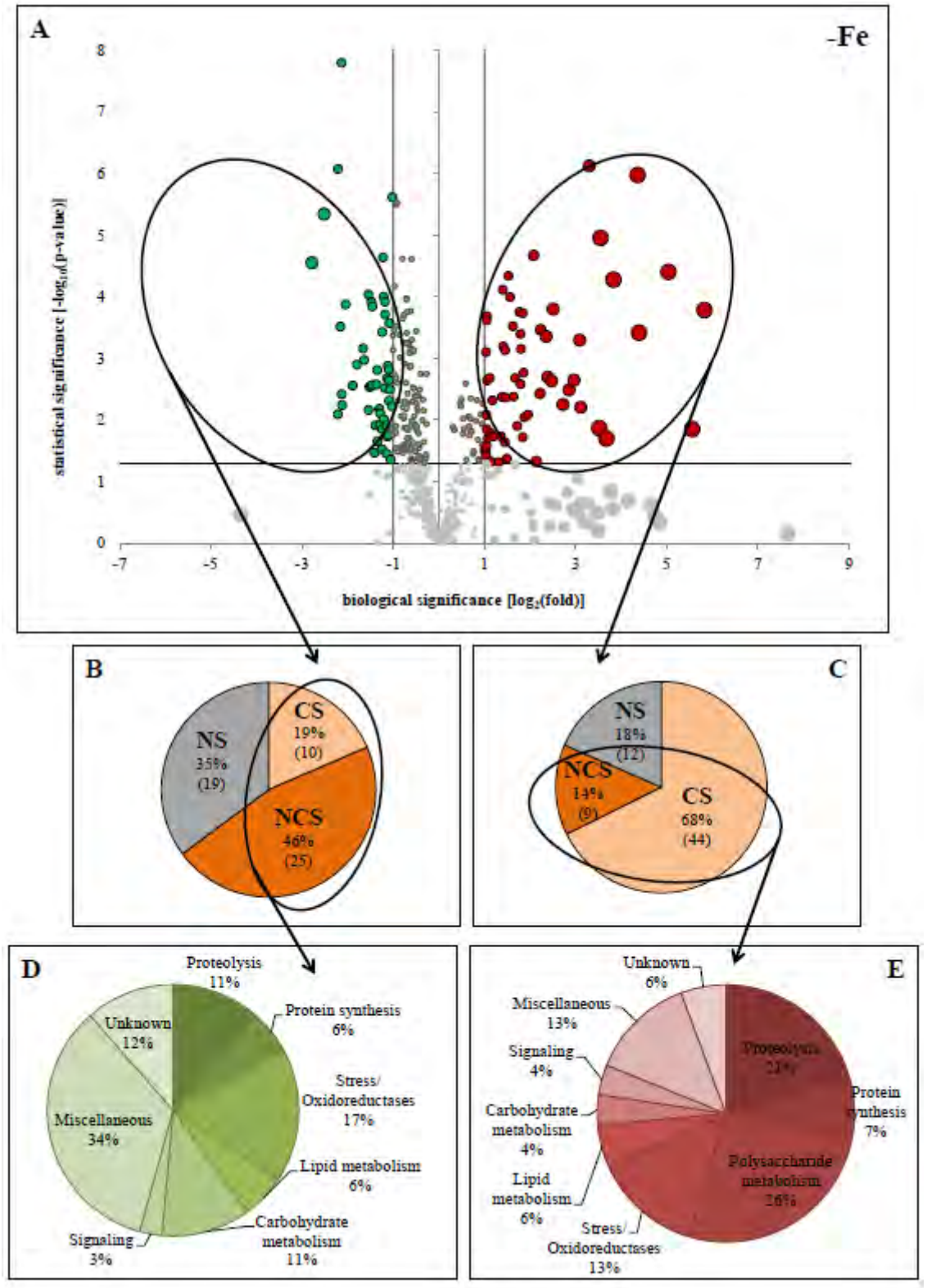

Fig. 1

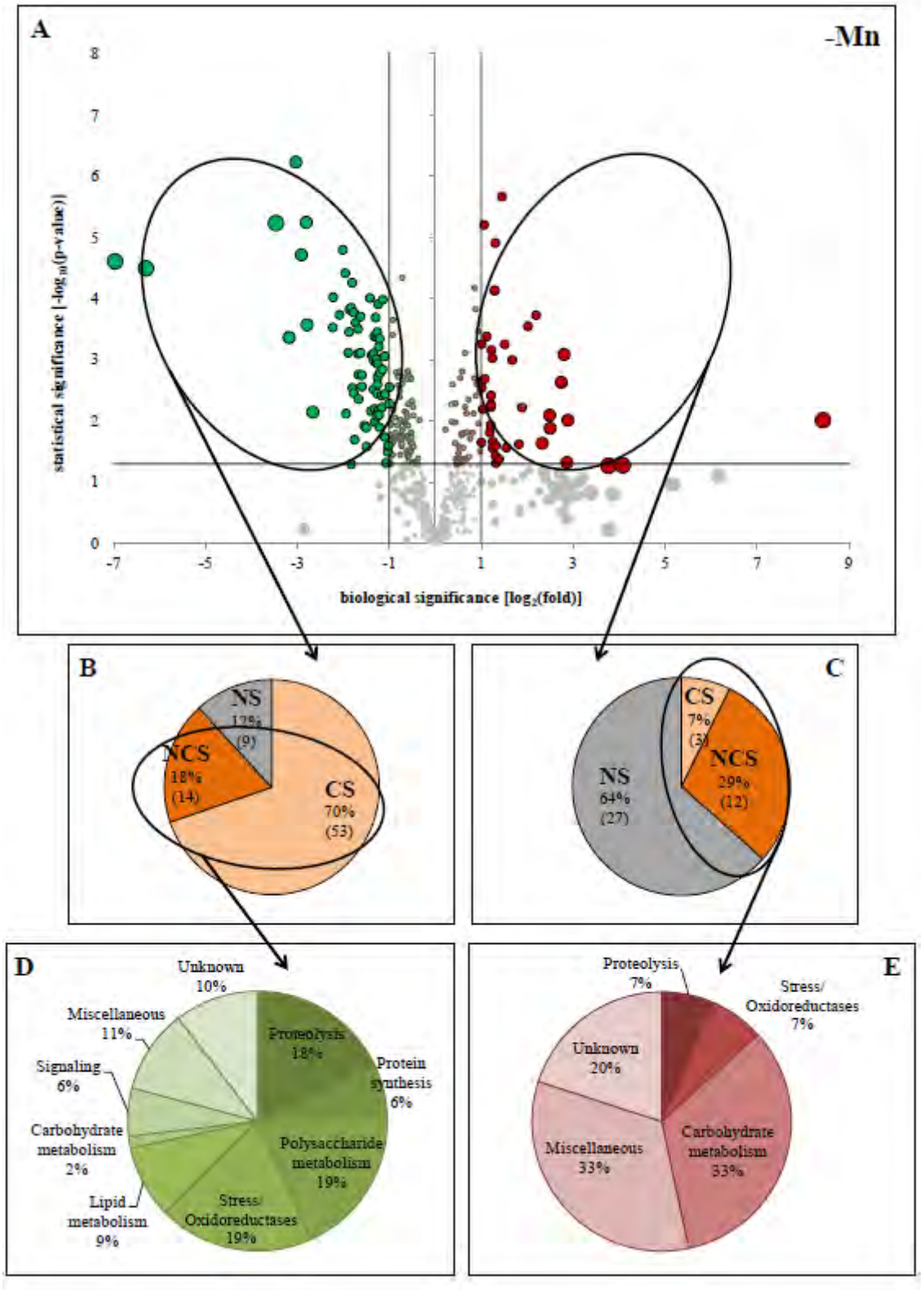

Fig. 2

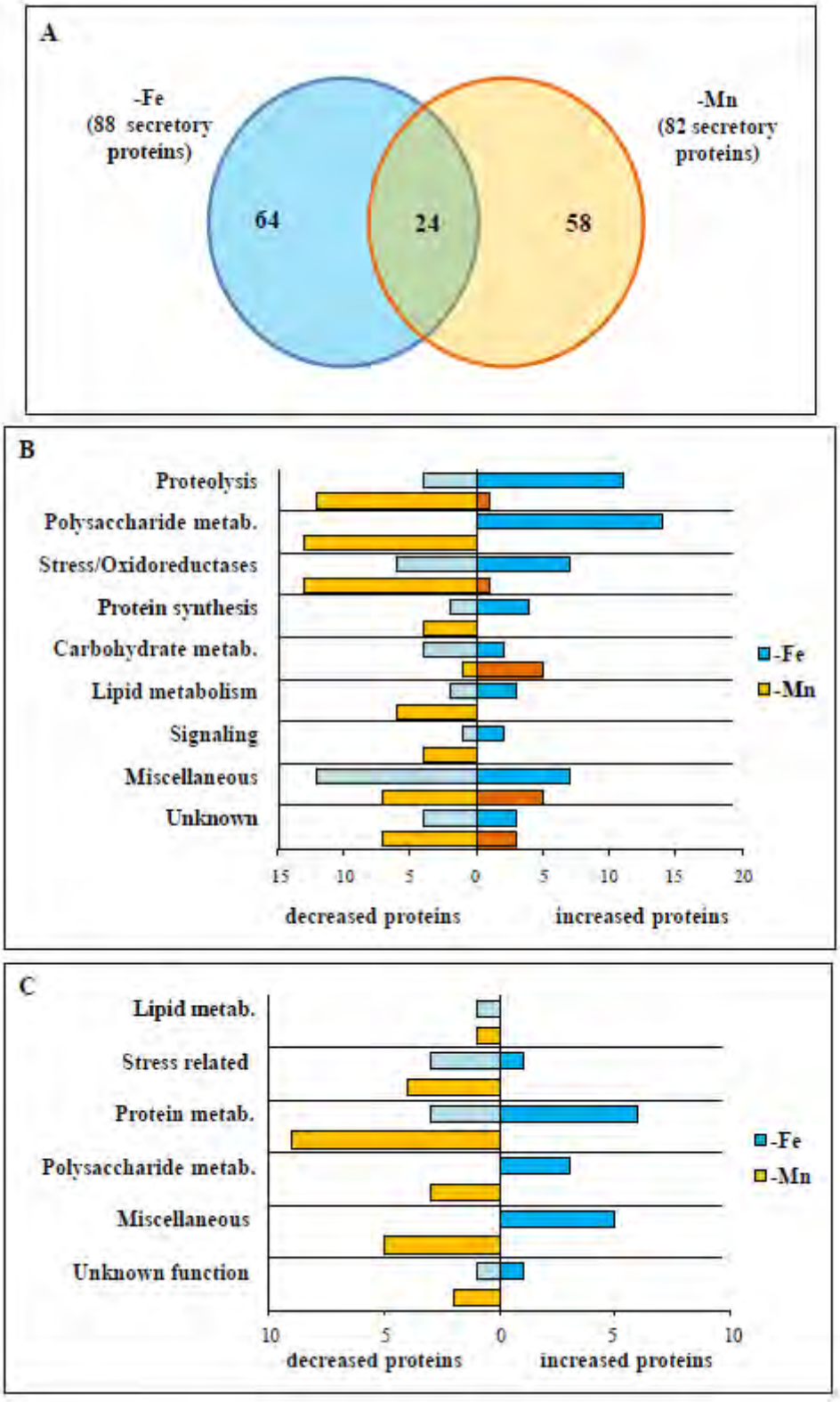

Fig. 3

SIGNIFICANCE

In spite of being essential for the delivery of nutrients to the shoots, our knowledge of xylem responses to nutrient deficiencies is very limited. The present work applies a shotgun proteomic approach to unravel the effects of Fe and Mn deficiencies on the xylem sap proteome. Overall, Fe deficiency seems to elicit more stress in the xylem sap proteome than Mn deficiency, based on the changes measured in proteolytic and oxido-reductase proteins, whereas both nutrients exert modifications in the composition of the primary and secondary cell wall. Cell wall modifications could affect the mechanical and permeability properties of the xylem sap vessels, and therefore ultimately affect solute transport and distribution to the leaves. Results also suggest that signaling cascades involving lipid and peptides might play a role in nutrient stress signaling and pinpoint interesting candidates for future studies. Finally, both nutrient deficiencies seem to affect phosphorylation and glycosylation processes, again following an opposite pattern.

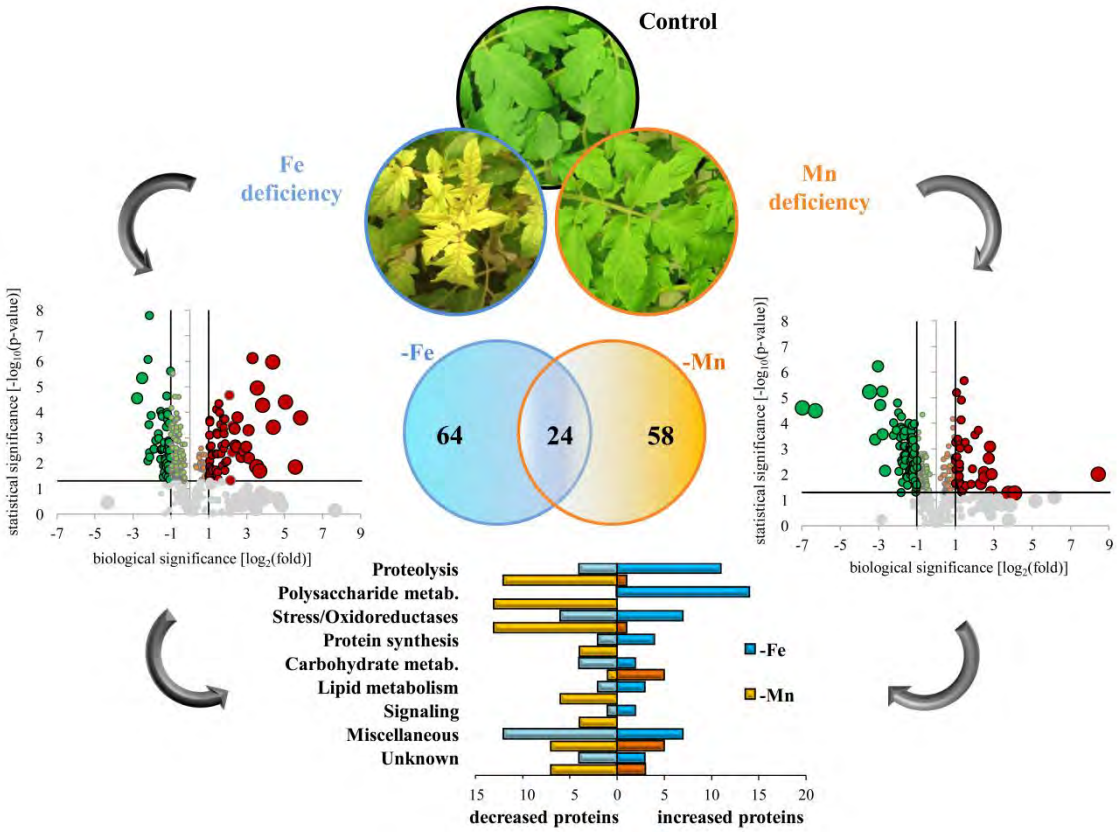

Graphical abstract

HIGHLIGHTS

- Oxidative, proteolytic enzyme abundances change more with Fe than with Mn shortage
- Both stresses lead to opposite changes in primary cell wall related proteins
- Both stresses lead to changes in secondary cell wall related proteins
- Pathways involving peptides and lipids seem involved in nutrient stress signaling
- Both stresses lead to opposite changes in phosphorylation/glycosylation proteins